

# Analysis Note of the Experiment

## Measurement of particle production with Roman Pot detectors in diffractive proton-proton interactions at $\sqrt{s} = 200$ GeV

Leszek Adamczyk<sup>1</sup> and Łukasz Fulek<sup>1</sup>

<sup>1</sup>*AGH University of Science and Technology, Kraków, Poland*

June 6, 2018

### Abstract

In this note we present the analysis of inclusive diffraction, focusing on the spectra of identified charged particles as pions, kaons and protons and their anti-particle counterparts in Single Diffraction ( $p + p \rightarrow p + X$ ) and Central Diffraction ( $p + p \rightarrow p + X + p$ ) processes. Moreover, the  $\bar{p}/p$  ratio as a function of rapidity is presented to study the baryon number transfer from forward to midrapidity in Single Diffraction. Similar effect has been studied in proton-proton and proton-photon interactions but it is the first measurement in proton-Pomeron interaction. This data come from proton-proton collisions collected in 2015. The forward proton(s) were tagged in the STAR Roman Pot system while the identified charged particle tracks were reconstructed in the STAR Time Projection Chamber (TPC). Ionization energy loss and time-of-flight of charged particles were used for particle identification.

We describe all stages of the analysis involving the extraction of efficiency and acceptance corrections, comparison of the data with MC simulations and systematic uncertainty studies.

*DRAFT*

# Contents

<b>1</b>	<b>Introduction</b>	<b>4</b>
1.1	Diffractive interactions in $pp$ collisions . . . . .	4
1.2	Baryon number transfer . . . . .	4
<b>2</b>	<b>Data set</b>	<b>6</b>
2.1	Bad runs . . . . .	6
<b>3</b>	<b>Analysis</b>	<b>7</b>
3.1	Forward proton selection . . . . .	7
3.2	Event and track selection . . . . .	7
3.2.1	Event selection . . . . .	7
3.2.2	Track selection . . . . .	7
3.3	Accidental background study . . . . .	7
3.3.1	Proton overlay probability . . . . .	7
3.3.2	Accidental background in SD . . . . .	8
3.3.3	Accidental background in CD . . . . .	10
3.3.4	TPC related distributions with additional proton selection cuts . . . . .	15
3.4	Particle Identification . . . . .	16
<b>4</b>	<b>Acceptance and Efficiency</b>	<b>17</b>
<b>5</b>	<b>Systematic uncertainty study</b>	<b>18</b>
<b>6</b>	<b>Results</b>	<b>19</b>
	<b>References</b>	<b>19</b>

# 1. Introduction

## 1.1 Diffractive interactions in $pp$ collisions

Diffractive processes at high energies are characterized by the exchange of the Pomeron, a color singlet object with quantum numbers of the vacuum described by the Regge theory [1][2]. Due to non-perturbative nature of interactions, there are difficulties in applying QCD to diffraction. Experimentally, diffraction is identified as interaction with large rapidity gap, i.e. final states are separated in rapidity space.

There are two processes of interest, shown in Figure 1.1 (a, b), the Central (CD:  $p + p \rightarrow p + X + p$ ) and Single (SD:  $p + p \rightarrow p + X$ ) Diffractive scattering, where  $X$  is the diffractive system. In CD interactions, two protons stay intact after the scattering, whereas in SD only one proton. The identified charged particle pro-

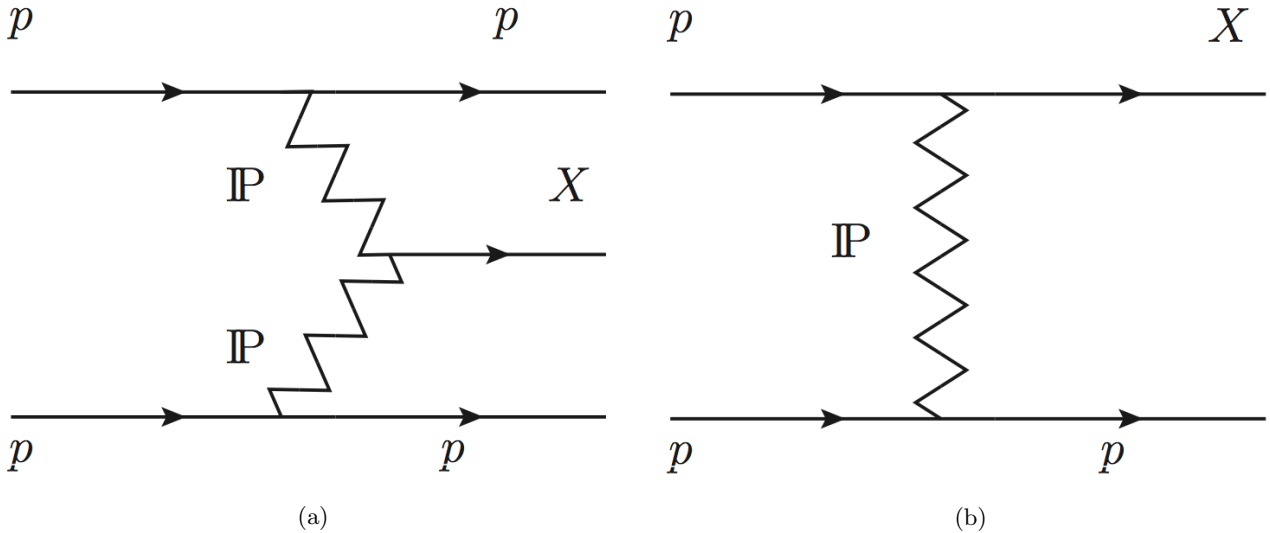


Figure 1.1: Diagrams of Central Diffraction (a) and Single Diffraction (b).

duction in the mid-rapidity region has been widely studied in minimum bias inelastic hadron-hadron collisions starting from the very first experiments performed at ISR at CERN throughout contemporary measurements with very high center-of-mass energy at RHIC [3] and LHC [4]. This is the first measurement with tagged forward protons, which allows efficient identification of diffractive events. The measured particle yields and ratios deliver information on collision dynamics and allows to validate some phenomenological models and tune some general purpose MC generators.

## 1.2 Baryon number transfer

In the Standard Model the baryon number is conserved in all interactions. The conserved baryon number associated with the beam particles is called "baryon number transfer" and has been studied theoretically for some time [5, 6, 7]. The baryon number transfer, which is quantified by the baryon to anti-baryon ratios, is often described as a function of the size of the transport in rapidity represented by rapidity difference  $\Delta y = y_{beam} - y$ , where  $y_{beam} = \ln(\sqrt{s}/m_p)$  is the rapidity of the beam and  $y$  the rapidity of the particles produced in the central system. In the String Junction Model [6] the baryon number can be transferred over large distances in the rapidity. In this picture, baryon number transfer is exponentially suppressed as a function of the rapidity interval  $\Delta y$ . In particular, when there are only purely gluonic exchanges between the valence quarks of the proton, the baryon number transfer does not depend on the rapidity and approaches a constant and finite value [5]. There is also a model [7], in which the initial baryon may end up at the backward end of the diffractive system. The edge of the rapidity gap  $\Delta\eta$  is related to the relative proton momentum loss  $\xi = \Delta E/E$ ,  $\Delta\eta \approx -\ln \xi = -\ln(M_X^2/s)$ . Therefore, the measurement of particle ratios as a function of  $\xi$  of the outgoing

protons should be taken into account to validate this model. There is a large number of the experimental data available on baryon number transfer [8]. The mid-rapidity anti-proton to proton ratio is sensitive to center-of-mass energy and varies between 0.4 for ISR energies and almost 1 for the LHC, where the transfer size in the rapidity space  $\Delta y$  is large and equals to almost 9 units. In addition, this effect was also measured by the H1 Collaboration in proton-photon interactions [9], where the data show that there is a sizeable baryon to anti-baryon asymmetry. The similar effect can be studied in SD interactions, where the direction of the initial baryon is uniquely defined.

## 2. Data set

### 2.1 Bad runs

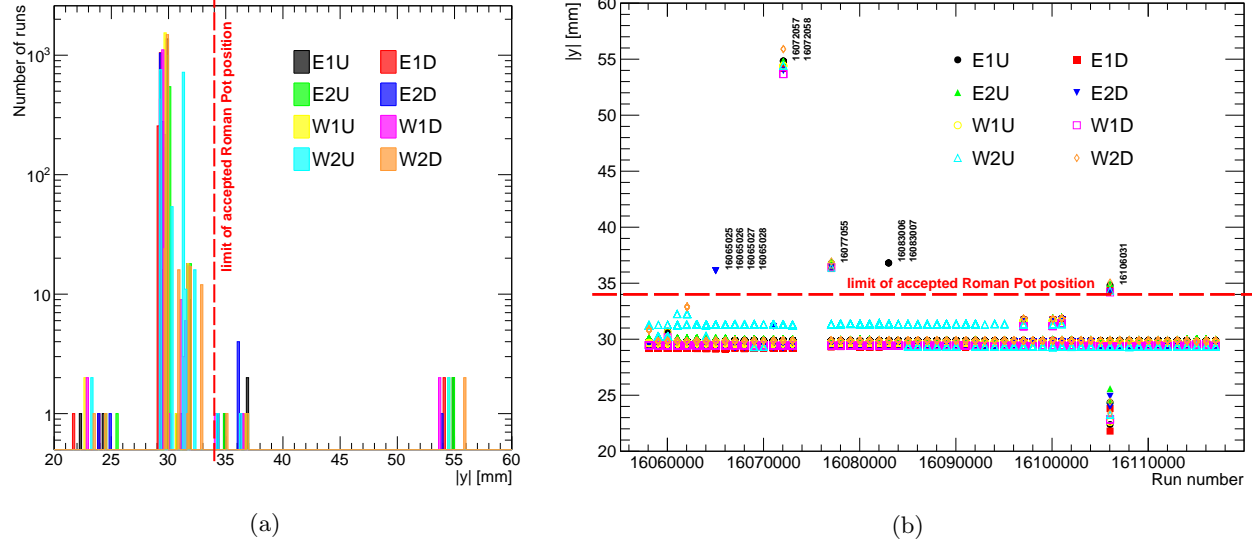


Figure 2.1: map of elastic proton hits in .

# 3. Analysis

## 3.1 Forward proton selection

## 3.2 Event and track selection

### 3.2.1 Event selection

### 3.2.2 Track selection

## 3.3 Accidental background study

The accidental backgrounds (same bunch pile-up background) are quantified using data-driven method. This includes any single(double)-side proton signal collected in coincidence with a diffractive like signal in the TPC-TOF detector. This type of background may come from the overlap of:

1. RP:

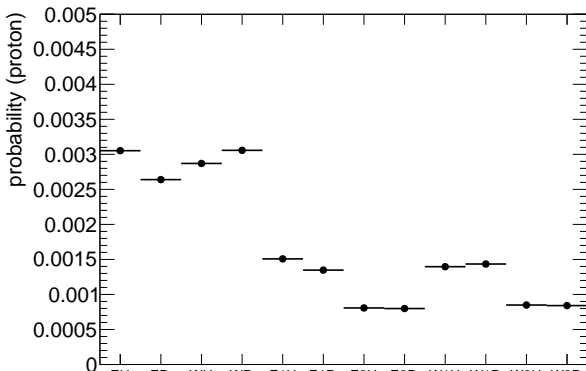
- proton from beamhalo,
- low mass SD process without activity in TOF,
- elastic or low mass CD processes with undetected proton on the other side,

2. TPC+TOF:

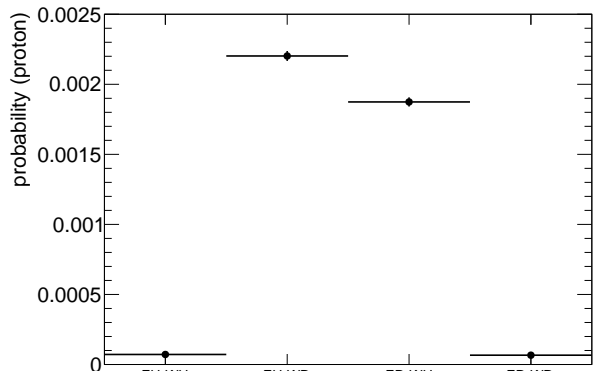
- any central activity (dominantly from ND events).

### 3.3.1 Proton overlay probability

The probability of observing the protons passing the RP proton track selection of the analysis was calculated from **Zerobias** trigger sample. As being assumed to be uncorrelated to the TPC-TOF activity, the probability is used to quantify the addition of an extra-proton to any kind of events. Figure 3.1a shows the derived probabilities of getting global and local proton tracks in SD. The probabilities of observing two protons on the opposite sides of the IP in CD using only proton global tracks were shown in the Figure 3.1b. The main contribution to the accidental background in CD comes from the inelastic RP configuration, where it is dominated by elastic (halo), elastic and SD, halo and SD protons and its probability equals to about 0.2%.



(a)



(b)

Figure 3.1: Proton overlay probability calculated from **Zerobias** trigger sample for SD (a) and CD (b, only proton global tracks used). The probability to observe accidental global tracks in RP in SD varies between 0.25 – 0.3%. Most of the accidental background in CD comes from the inelastic RP configuration.

### 3.3.2 Accidental background in SD

The background from accidentals in SD events was calculated from the **Zerobias** sample multiplied by the probability of observing the accidental proton track in the RP and corrected by the relevant trigger prescales  $\frac{PS_{Zerobias}}{PS_{SDT}}$ . Figure 3.2 shows the proton hit position in E1U with the data-driven background contribution for the region of interest (a,b - proton global and local tracks; c,d - only proton global tracks). Due to observe the

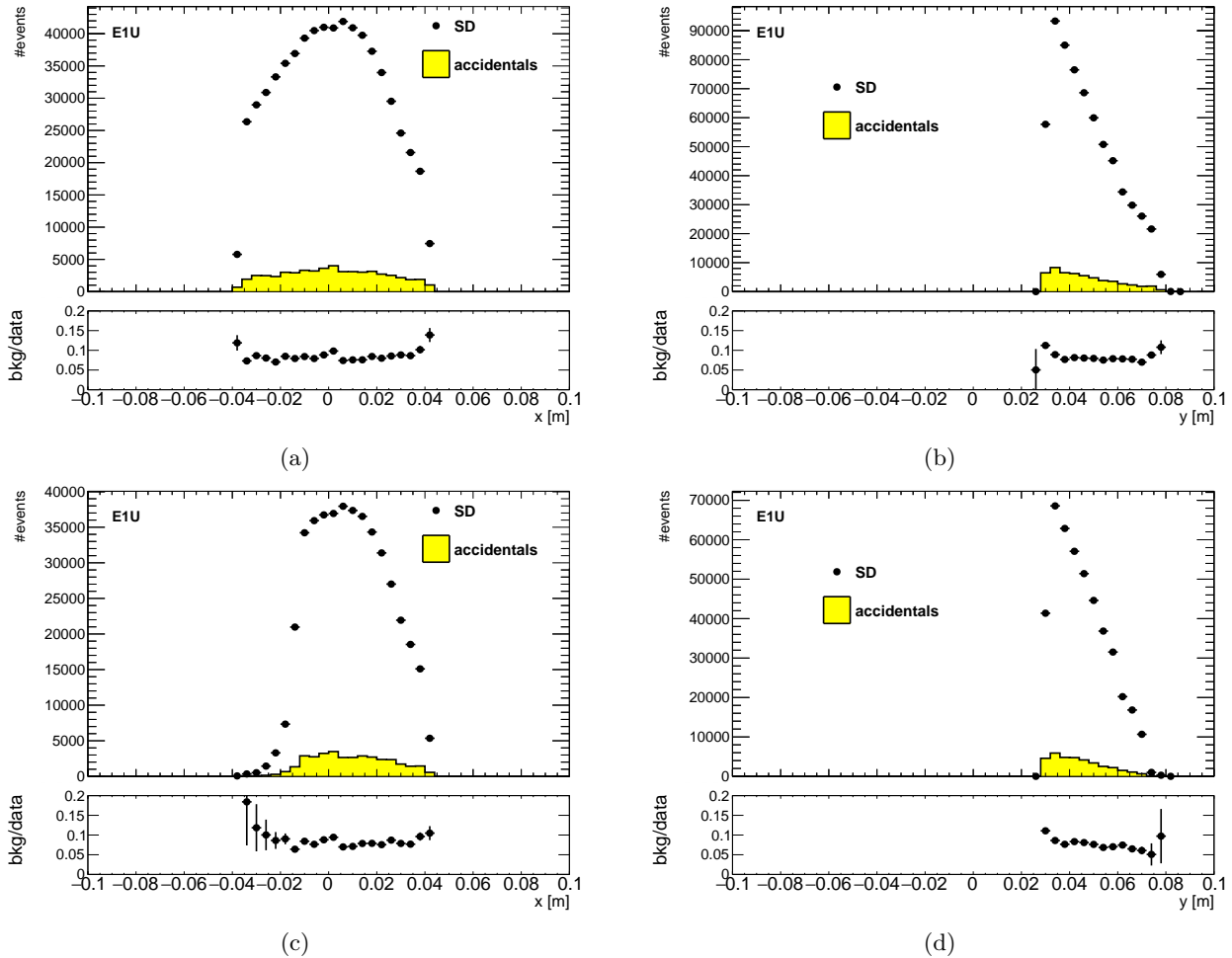


Figure 3.2: Proton hit position in SD using global+local proton tracks (a-b) and only global proton tracks (c-d). The background contribution equals to about 10%.

same accidental background contribution for global and global+local proton track ( $\approx 10\%$ ), also the  $-t$  and  $\xi$  distributions were checked (Figure 3.3). To reconstruct properly  $-t$  and  $\xi$  only global proton tracks were used. The flat background was observed in the  $-t$  distribution. However, the  $\xi$  distribution shows that most of the background is located around  $\xi \approx 0$ , which confirms the assumption that most of the accidental background comes from elastic, beam halo or low mass diffractive protons.

Additionally, the background begins to rise at  $\xi \approx 0.4$ . This probably comes from true or fake tracks reconstructed in RP arising from showers happening outside the RP stations. Finally, the additional proton selection cuts were obtained for SD - the proton track is required to be a global track with  $0.02 < \xi < 0.4$ . The probability to observe the accidental proton in RP decreased to about 0.15% (Figure 3.4a) and the accidental background contribution is about 5 – 10% (Figure 3.4b).

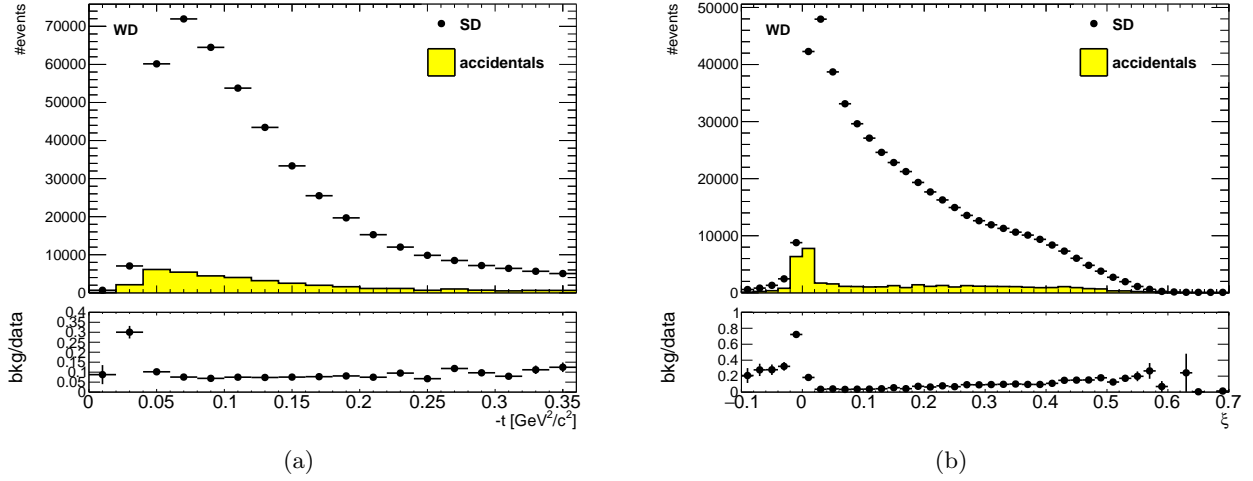


Figure 3.3:  $-t$  and  $\xi$  distribution for WD arm in SD. Accidental background suppressed for  $0.02 < \xi < 0.4$ .

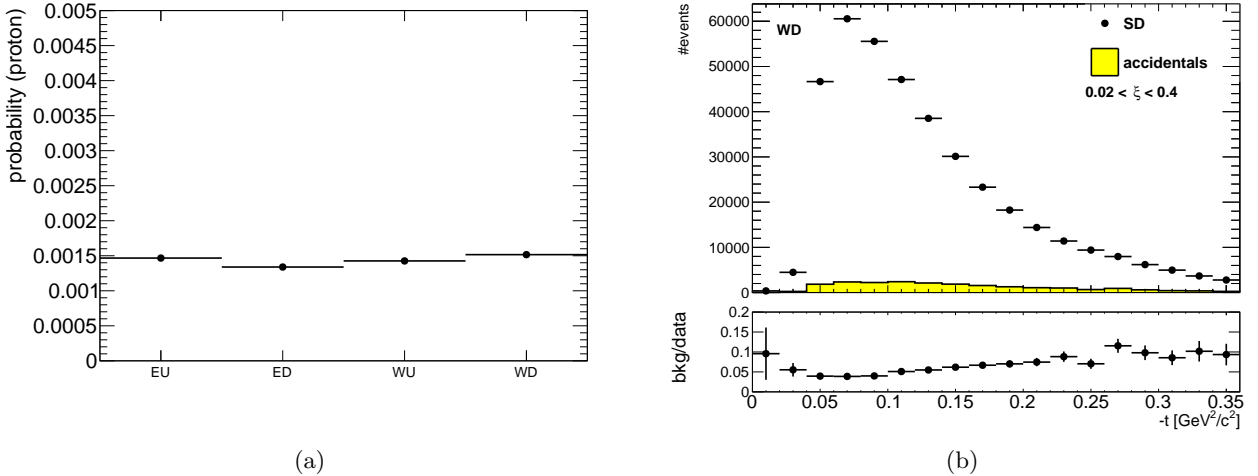


Figure 3.4: Proton overlay probability (a) and  $-t$  (b) distribution for SD events with  $0.02 < \xi < 0.4$ . The probability to observe accidental proton in RP decreased to about 0.15%.

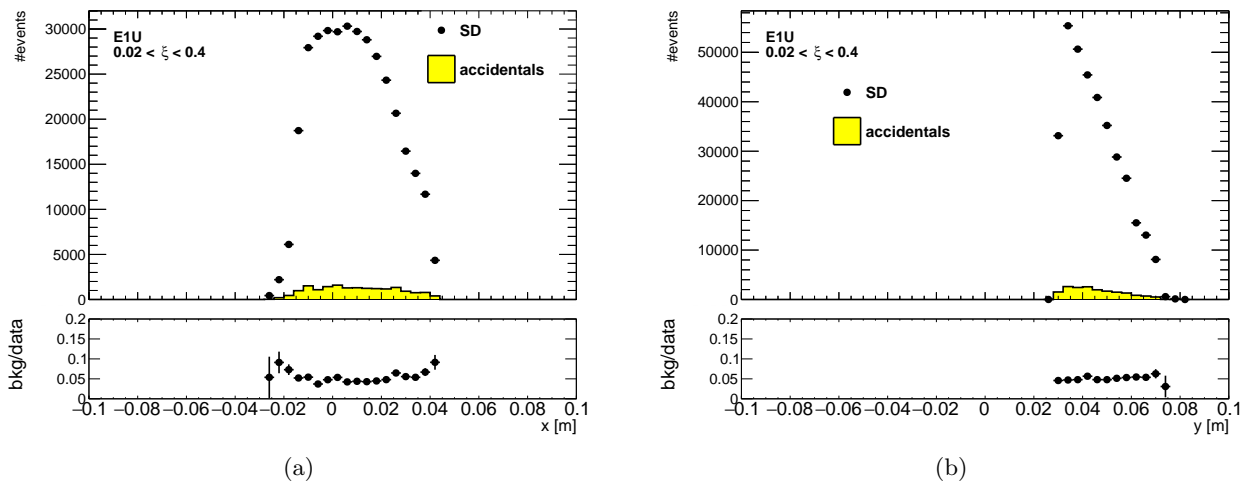


Figure 3.5: Proton hit position in E1U for SD events with  $0.02 < \xi < 0.4$ .

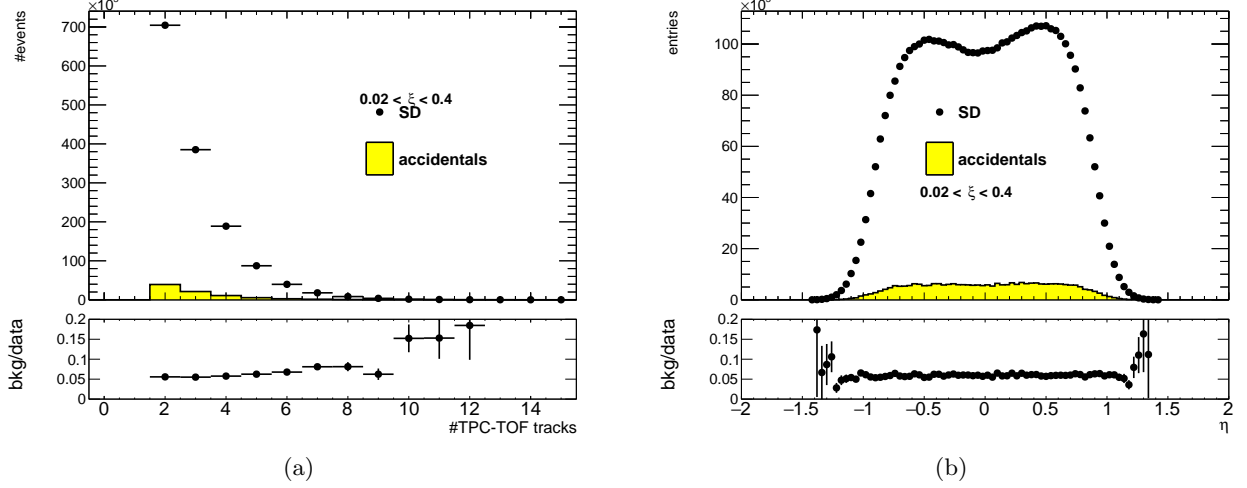


Figure 3.6: TPC-TOF related variables (TPC-TOF track multiplicity and  $\eta$  of those tracks) for SD events with  $0.02 < \xi < 0.4$ . The background contribution is about 5 – 10%.

### 3.3.3 Accidental background in CD

The background from accidents in CD events was calculated in the similar way to the SD. Only proton global tracks were used to calculate the probability of observing two accidental protons on the opposite sides of the IP. Figure 3.7 shows the collinearity distributions for inelastic (a) and elastic (b) RP configuration.

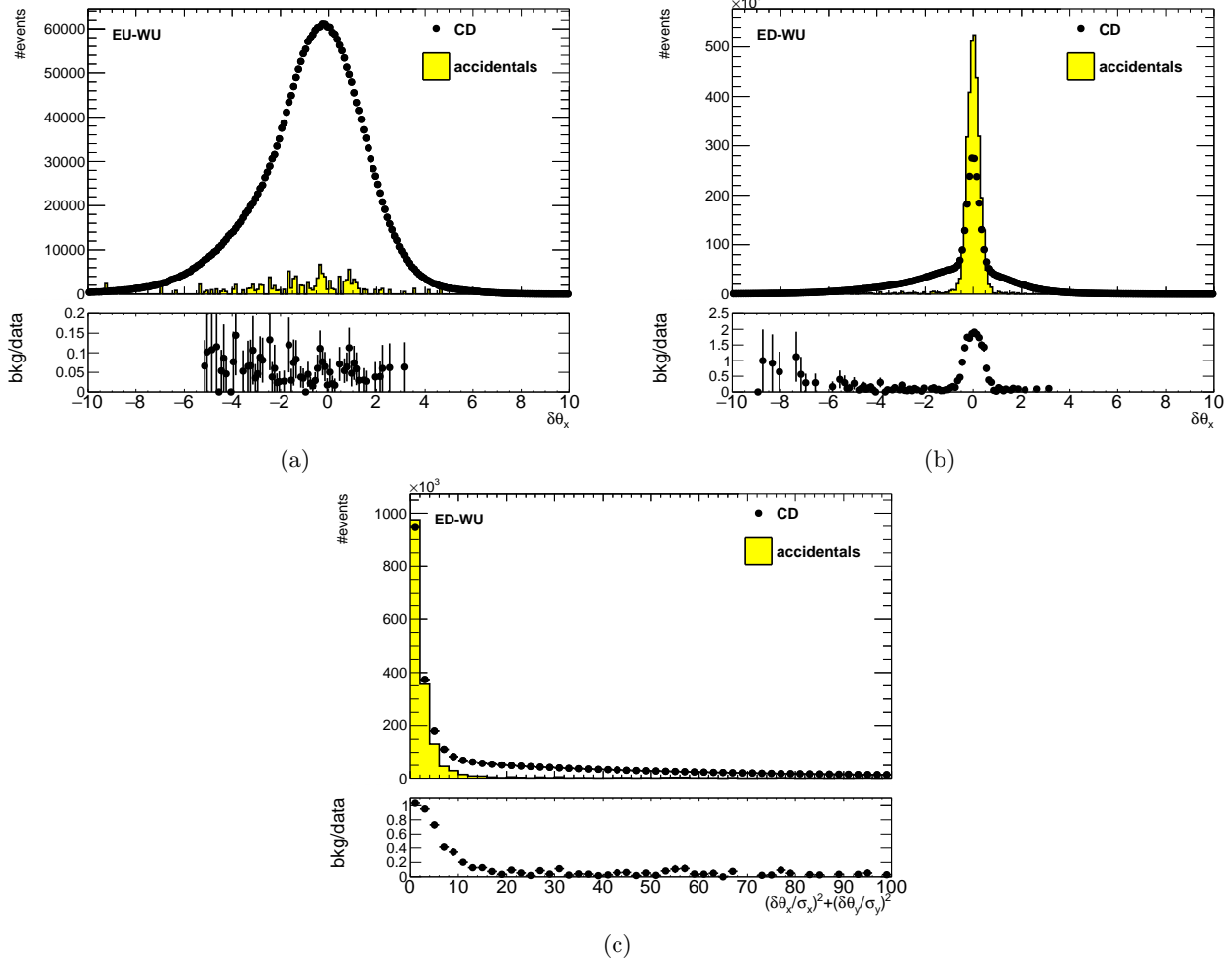


Figure 3.7: Collinearity distribution  $\theta_X$  for inelastic (a) and elastic (b) RP configuration in CD. The accidental background for elastic configuration is overestimated. The background was normalized to the signal in the first bin of the collinearity distribution (c).

The accidental background for the elastic configuration excess the 100% and is overestimated. Two solutions were found to estimate the background in the elastic RP configuration:

1. Require the protons to be anti-collinear  $\left( (\delta\theta_x/\sigma_x)^2 + (\delta\theta_y/\sigma_y)^2 < 3^2 \right)$ .

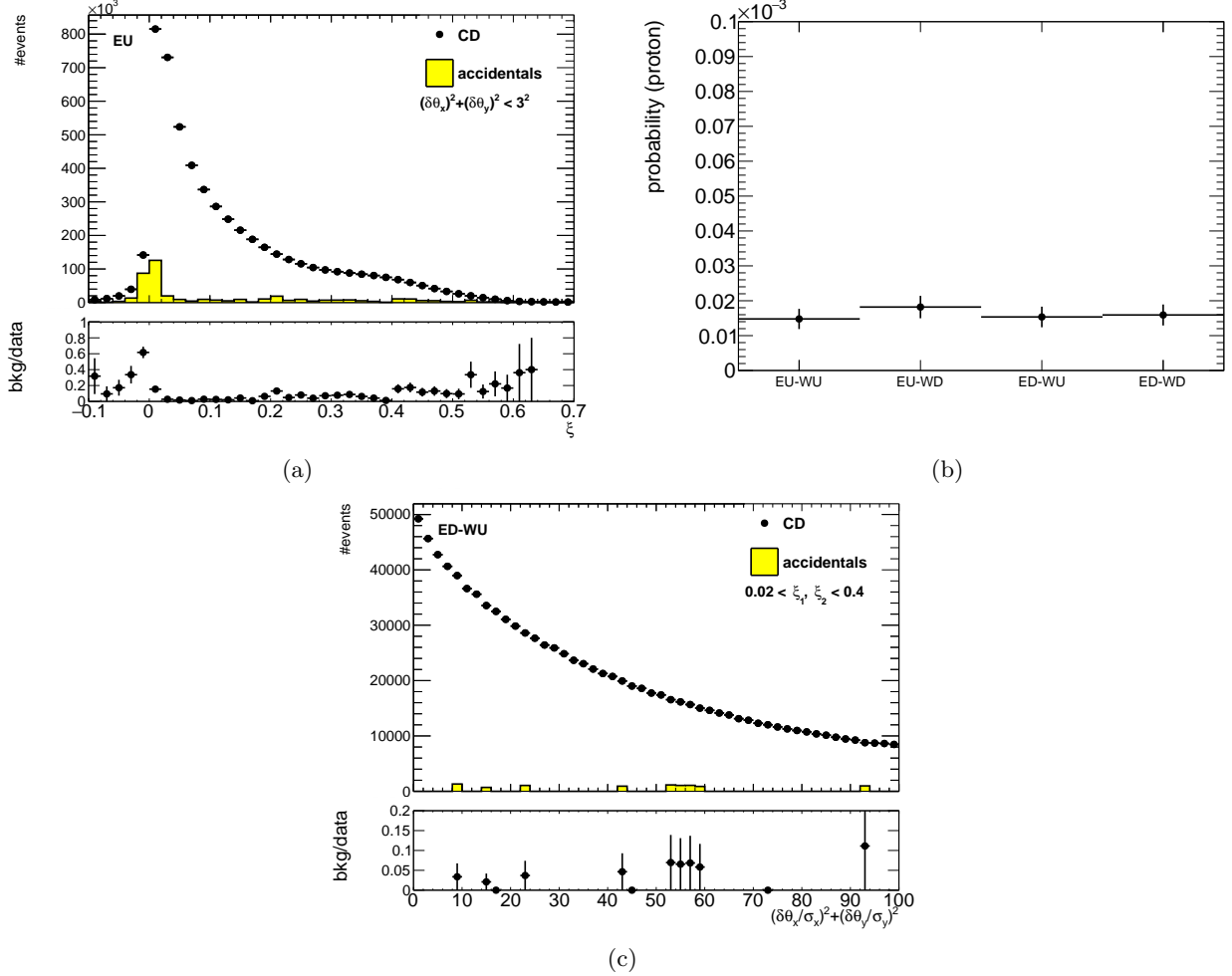


Figure 3.8:  $\xi$  distribution of protons in EU arm with collinearity cut. The background is suppressed for  $0.02 < \xi_1, \xi_2 < 0.4$  and the proton overlay probability is reduced to  $2 \cdot 10^{-5}$ . The accidental background contribution was reduced to about 5% with this cut.

The  $\xi$  distribution with collinearity cut, as shown in Figure 3.8a, was checked and it was found that the proton tracks should be required to be global tracks with  $0.02 < \xi_1, \xi_2 < 0.4$ . With this cuts the probability of observing two accidental protons was reduced to about  $2 \cdot 10^{-5}$  for all RP configurations (Figure 3.8b). Additionally, the overestimation of the background was not observed in the collinearity distribution (Figure 3.8c) and the accidental background contribution decreased to about 5%.

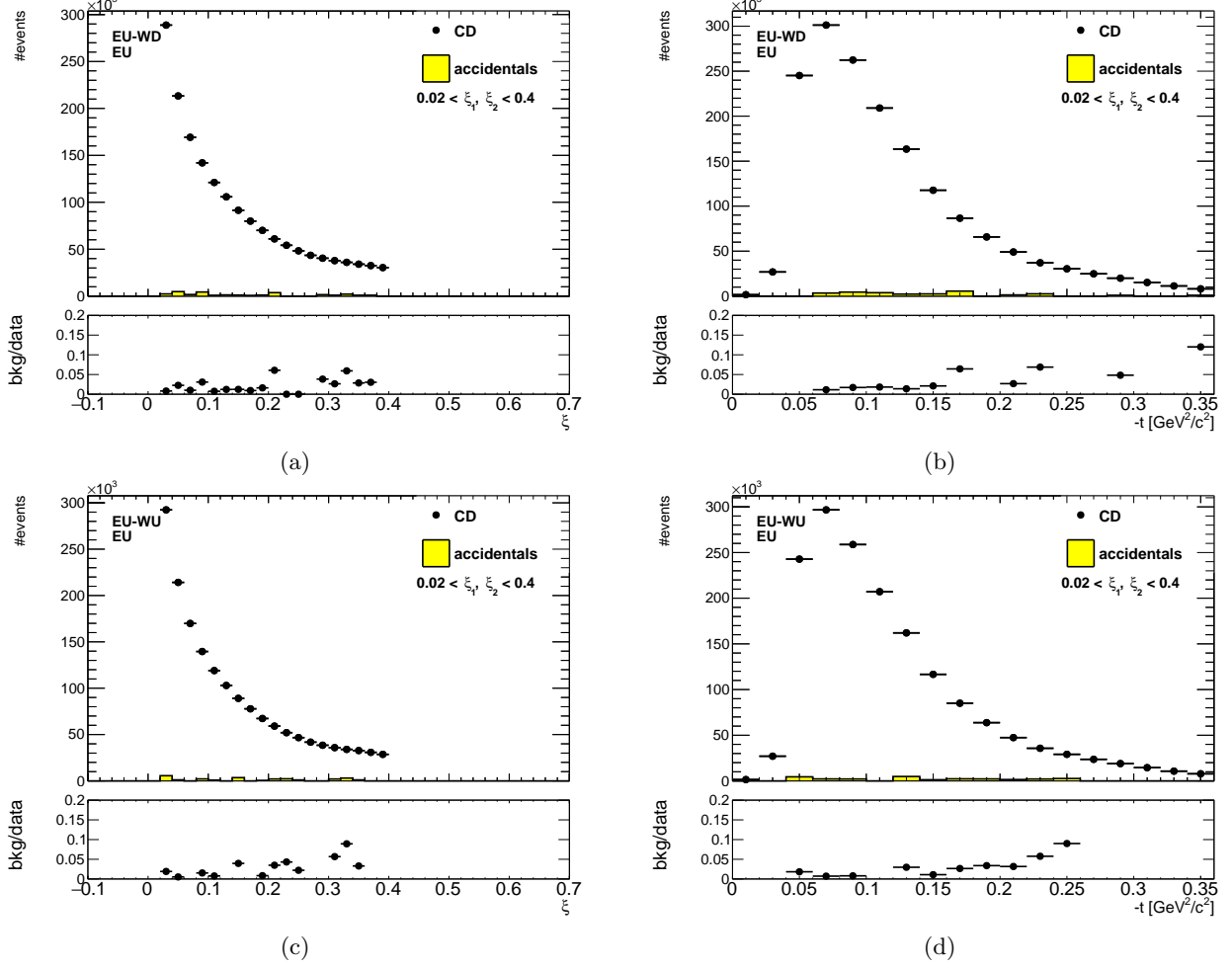


Figure 3.9:  $\xi$  and  $-t$  in elastic and inelastic RP configuration measured with EU. The background is reduced to about 5% in both RP configurations.

2. Normalize the background to the signal in the first bin of the collinearity distribution (Figure 3.7c). Here it was assumed that all collinear protons are background protons and the upper limit for the background was set. Also the scale factor for the background was found. Similar to the first method, it was found that the background is suppressed for  $0.02 < \xi_1, \xi_2 < 0.4$  and varies between 2 – 3% (Figure 3.10 b-d). The collinearity cut is not required anymore.

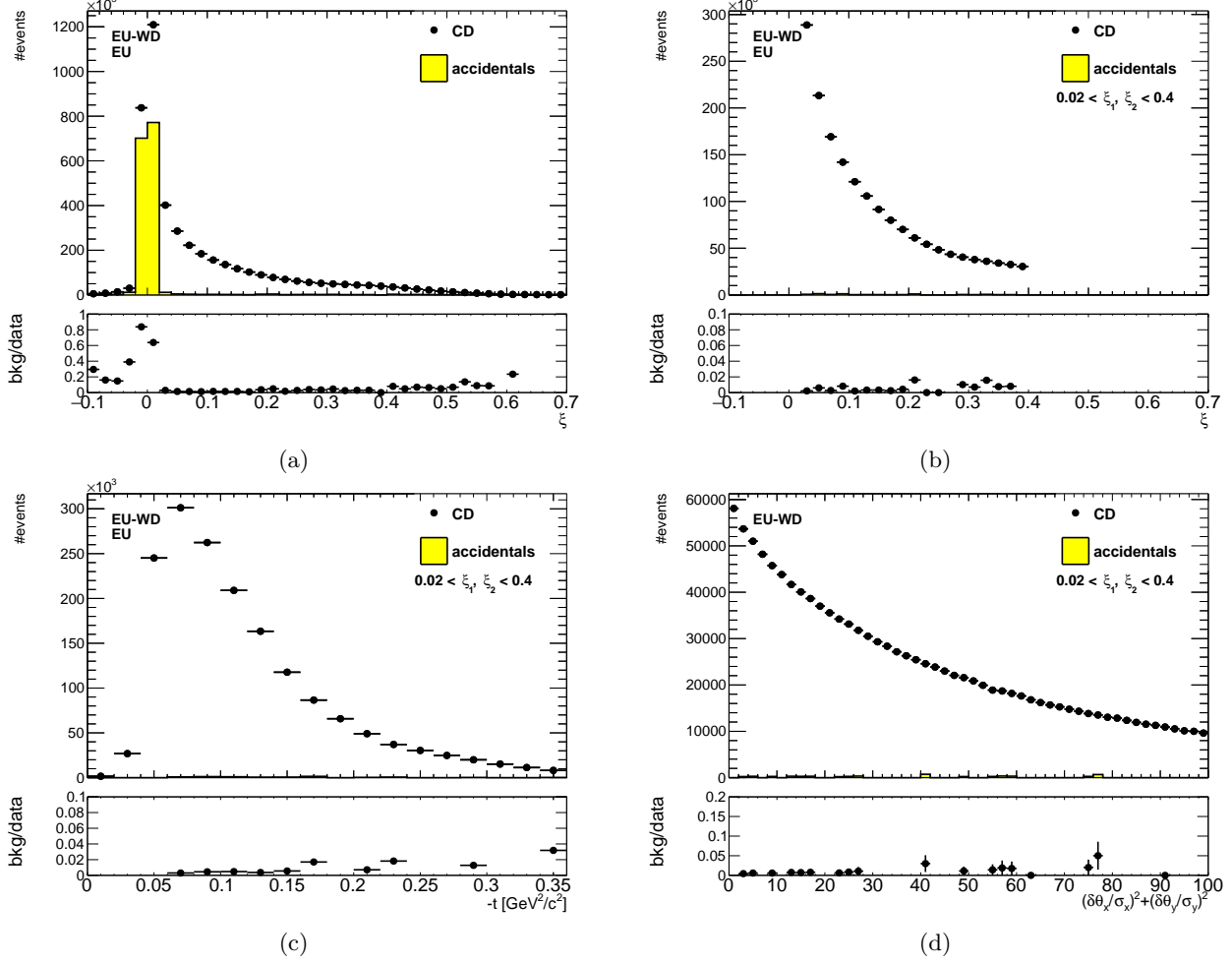
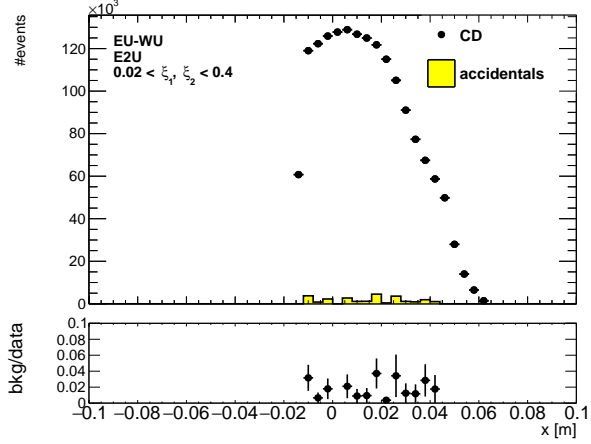
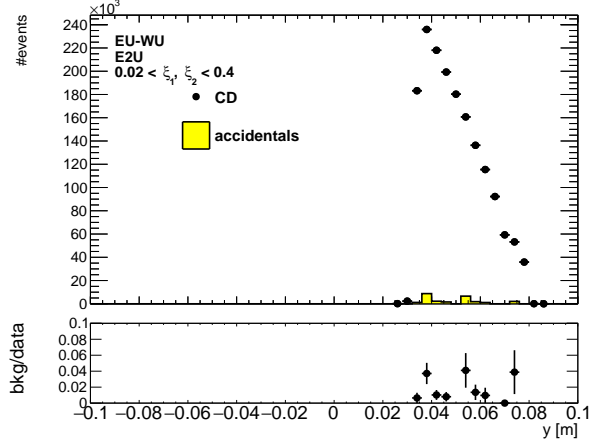


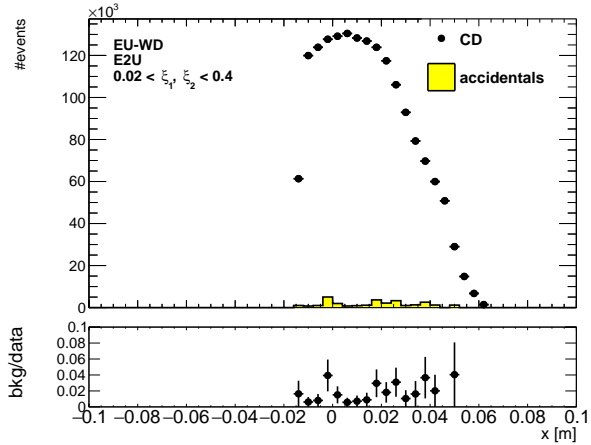
Figure 3.10:  $\xi$  distribution in CD with the accidental background normalized to the signal in the first bin of the collinearity distribution (Figure 3.7c). Most of the accidental background located outside the  $0.02 < \xi_1, \xi_2 < 0.4$  region. The background reduced to about 2 – 3% in  $\xi$ ,  $-t$  and collinearity distributions with  $0.02 < \xi_1, \xi_2 < 0.4$  cut applied.



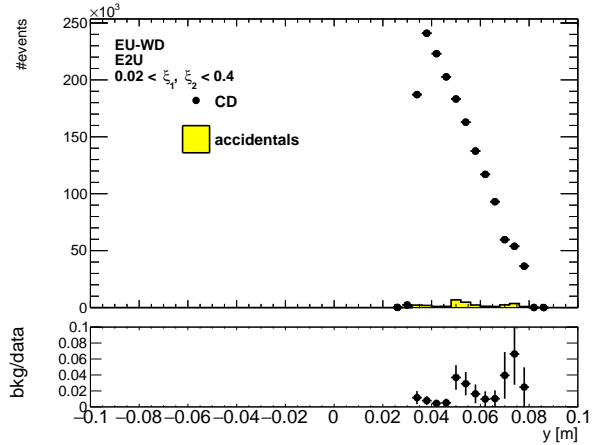
(a)



(b)

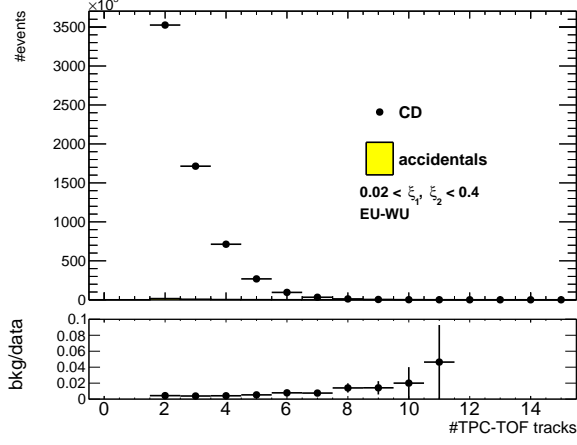


(c)

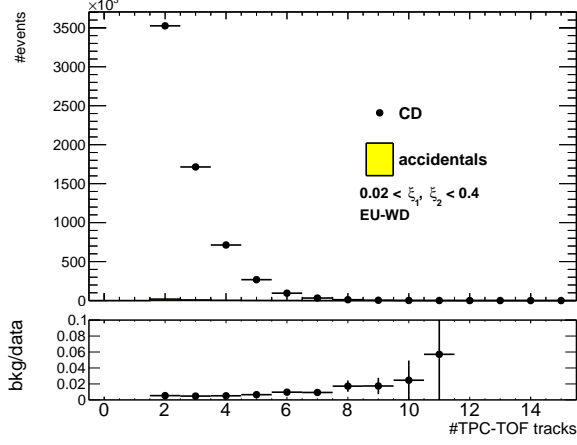


(d)

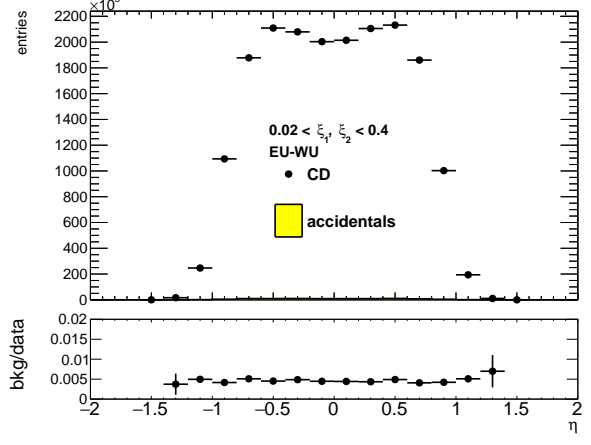
Figure 3.11: Proton hit positions for E2U in inelastic (a, b) and elastic (c,d) RP configuration with  $0.02 < \xi_1, \xi_2 < 0.4$  cut applied. The background reduced to about 2 – 4% in both RP configurations.



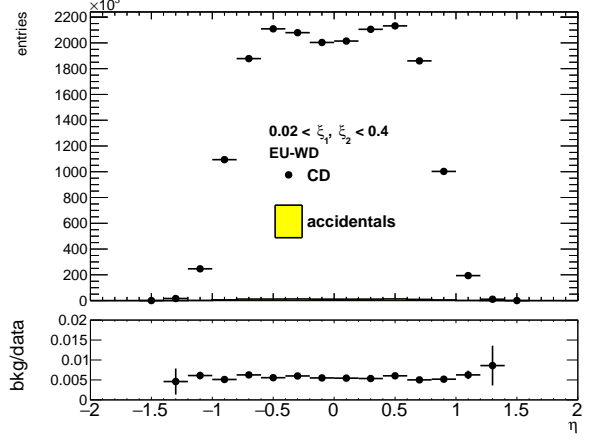
(a)



(c)



(b)



(d)

Figure 3.12: TPC-TOF related variables (TPC-TOF track multiplicity and  $\eta$  of those tracks) for CD events with  $0.02 < \xi_1, \xi_2 < 0.4$ . The background contribution is about 0.5%.

### 3.3.4 TPC related distributions with additional proton selection cuts

The additional proton selection  $\xi(\xi_1, \xi_2)$  cuts reduce the statistics of about 20% and 50% for SD and CD, respectively. The most significant background reduction was observed mainly in CD. Figure 3.13 shows the comparison of the  $p_T$  (c, f) and  $\eta$  (b, e) distributions with and without the  $\xi(\xi_1, \xi_2)$  cuts applied. In spite of the reduction of the background, the shape of those distributions did not change. Although, the TPC-TOF track multiplicity distribution changed with above cuts applied (Figure 3.13 a, d). The rest of the accidental background has to be subtracted statistically.

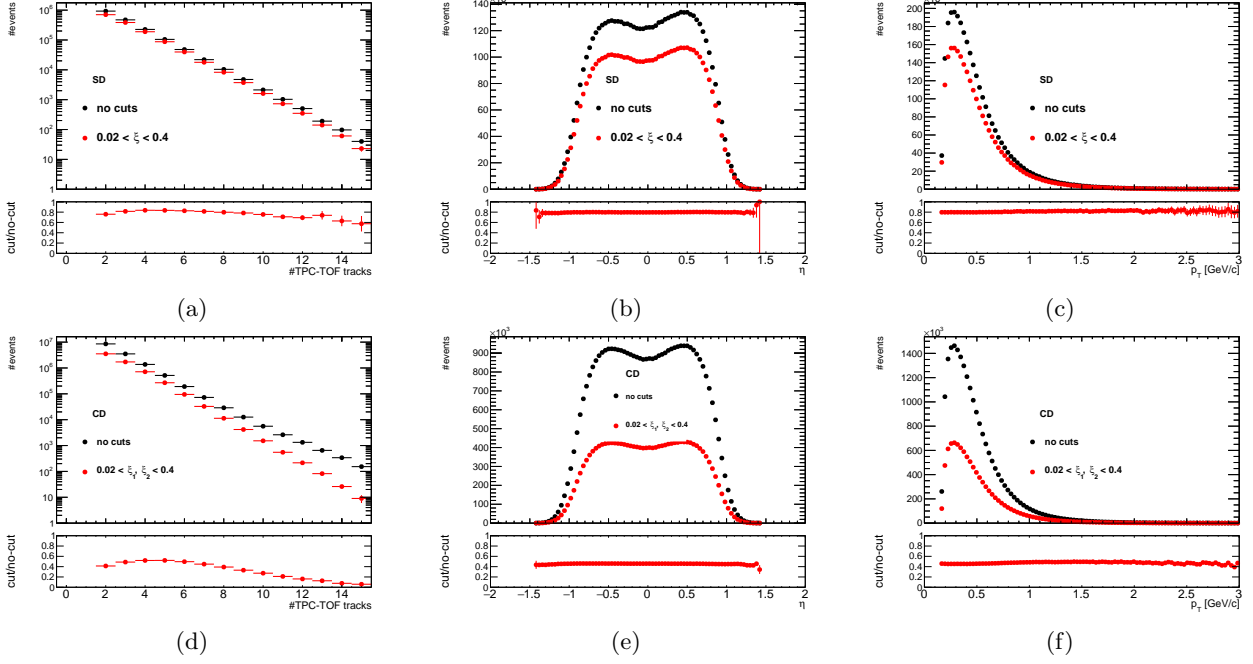


Figure 3.13: TPC-TOF related distributions with and without additional proton track selection cuts applied in SD (a-c) and CD (d-f). The additional proton selection  $\xi$  ( $\xi_1, \xi_2$ ) cuts reduce the statistics of about 20% and 50% for SD and CD, respectively.

### 3.4 Particle Identification

## 4. Acceptance and Efficiency

## 5. Systematic uncertainty study

## 6. Results

# References

- [1] V. Barone and E. Predazzi, *High-Energy Particle Diffraction*. Springer, 2002.
- [2] S. Donnachie, G. Dosch, P. Landshoff, and O. Nachtmann, *Pomeron Physics and QCD*. Cambridge Monographs on Particle Physics, Nuclear Physics and Cosmology. Cambridge University Press, 2002.
- [3] B. Abelev, M. Aggarwal, Z. Ahammed, B. Anderson, D. Arkhipkin, K. Krueger, H. Spinka, and D. Underwood, “Systematic measurements of identified particle spectra in pp, d+au, and au+au collisions at the star detector.,” *Physical Review C: Nuclear Physics* **79** (2009) –, 10.1103/PhysRevC.79.034909.
- [4] **ALICE** Collaboration, J. Adam *et al.*, “Measurement of pion, kaon and proton production in proton–proton collisions at  $\sqrt{s} = 7$  TeV,” *Eur. Phys. J.* **C75** no. 5, (2015) 226, [arXiv:1504.00024 \[nucl-ex\]](#).
- [5] B. Z. Kopeliovich and B. G. Zakharov, “Novel Mechanisms of Baryon Number Flow Over Large Rapidity Gap,” *Z. Phys.* **C43** (1989) 241.
- [6] G. C. Rossi and G. Veneziano, “A Possible Description of Baryon Dynamics in Dual and Gauge Theories,” *Nucl. Phys.* **B123** (1977) 507–545.
- [7] F. W. Bopp, “Central baryons in dual models and the possibility of a backward peak in diffraction,” [arXiv:hep-ph/0002190 \[hep-ph\]](#).
- [8] **ALICE** Collaboration, K. Aamodt *et al.*, “Midrapidity antiproton-to-proton ratio in pp collisions at  $\sqrt{s} = 0.9$  and 7 TeV measured by the ALICE experiment,” *Phys. Rev. Lett.* **105** (2010) 072002, [arXiv:1006.5432 \[hep-ex\]](#).
- [9] B. Kopeliovich and B. Povh, “Baryon stopping at HERA: Evidence for gluonic mechanism,” *Phys. Lett.* **B446** (1999) 321–325, [arXiv:hep-ph/9810530 \[hep-ph\]](#).
- [10] **STAR** Collaboration, K. H. Ackermann *et al.*, “STAR detector overview,” *Nucl. Instrum. Meth.* **A499** (2003) 624–632.
- [11] **STAR** Collaboration, W. J. Llope, “The large-area time-of-flight (TOF) upgrade for the STAR detector,” *AIP Conf. Proc.* **1099** (2009) 778–781.
- [12] **STAR** Collaboration, L. Adamczyk *et al.*, “Single Spin Asymmetry  $A_N$  in Polarized Proton-Proton Elastic Scattering at  $\sqrt{s} = 200$  GeV,” *Phys.Lett.* **B719** (2013) 62–69, [arXiv:1206.1928 \[nucl-ex\]](#).
- [13] **STAR** Collaboration, J. Kiryluk, “Relative luminosity measurement in STAR and implications for spin asymmetry determinations,” *AIP Conf. Proc.* **675** (2003) 424–428. [,424(2003)].
- [14] C. Adler, A. Denisov, E. Garcia, M. J. Murray, H. Strobele, and S. N. White, “The RHIC zero degree calorimeter,” *Nucl. Instrum. Meth.* **A470** (2001) 488–499, [arXiv:nucl-ex/0008005 \[nucl-ex\]](#).